EPJ Web of Conferences **90**, 06005 (2015)
DOI: 10.1051/epjconf/20159006005

Charmonium photoproduction in ultra-peripheral p-Pb and Pb-Pb collisions with ALICE at the LHC

D. De Gruttola[1,2,a]

[1] *Centro Studi e Ricerche e Museo Storico della Fisica "Enrico Fermi", Rome, Italy*
[2] *Salerno INFN, Complesso Universitario di Monte Sant'Angelo Via Cintia, Napoli, Italy*

Abstract. The photoproduction of vector mesons in Ultra-Peripheral Collisions (UPC) is a powerful tool to probe the nuclear gluon distribution (Pb-Pb collisions) and the gluon structure function in the proton (p-Pb collisions). The first measurements of coherent photoproduced J/ψ and ψ(2S) in Pb-Pb collisions at $\sqrt{s_{NN}}$ = 2.76 TeV, performed with the ALICE detector, are described and compared to STARLIGHT and QCD based models, in order to investigate nuclear gluon shadowing. The results of the measurement of exclusive J/ψ photoproduction off protons in p-Pb collisions at $\sqrt{s_{NN}}$ = 5.02 TeV are also presented.

1 Ultra-peripheral collisions

Ultra-peripheral collisions may occur when two accelerated nuclei are separated by impact parameters larger than the sum of their radii: hadronic interactions are strongly suppressed so that both pure electromagnetic and photonuclear processes can be studied. These interactions can be measured in Pb–Pb collisions at the LHC, where the available centre of mass energy per nucleon pair is 2.76 TeV, allowing $\gamma\gamma$ interactions at ≈80 GeV and γp at ≈480 GeV center of mass energy, to be compared with 10 and 30 GeV respectively, reached at RHIC. An accelerated charge can be considered as a source of quasi-real photons with virtuality Q^2 depending on the radius of the Pb nucleus and being ∼30 MeV^2, according to Fermi [1] and to relativistic approach by Weizs*ä*cker [2] and Williams [3]. One of these quasi-real photons may interact either with the opposite ion or with one of its quasi-real photons. The cross section for photon induced reactions is large because the strong electromagnetic field of the nucleus enhances the intensity of the virtual photon flux, which grows as Z^2, where Z is the charge of the nucleus. UPCs are characterized by the photoproduction of vector mesons (ρ^0, J/ψ, ψ', Υ,...) and by pure QED processes giving rise to a di-lepton continuum. The physics of ultra-peripheral collisions is reviewed in [4, 5].

2 Physics motivations

Exclusive photoproduction of vector mesons, where a vector meson is produced in an event with no other final state particles, is of particular interest. In Pb-Pb collisions these measurements probe nuclear gluon shadowing in the low Bjorken-x region, where it is poorly known. On the other hand, p-Pb collisions allow the study of the evolution with energy of the gluon distribution in the proton, and provide a powerful tool to investigate gluon saturation. ALICE can extend the measurement done at HERA [6, 7] and ZEUS [8] to higher γp center of mass energy.

2.1 Pb-Pb collisions

Exclusive photoproduction of vector mesons is expected to probe the nuclear gluon distribution [9], for which there is considerable uncertainty in the low-x region, as it can be seen in Fig.1, showing the ratio of their parton distribution functions for bounded and free protons [10, 11]. Exclusive photoproduction can be either coherent, if the photon couples coherently to all nucleons, or incoherent, if the photon couples to a single nucleon. Coherent production is characterized by low vector meson transverse momentum ($\langle p_T \rangle$∼60 MeV/c) and the target nucleus normally does not break up. Incoherent production, corresponding to quasi-elastic scattering off a single nucleon, is characterized by a higher transverse momentum ($\langle p_T \rangle$∼500 MeV/c) and the target nucleus normally breaks up; except for single nucleons or nuclear fragments in the very forward region no other particles are produced. In what follows, results on coherent J/ψ production in the forward region, reconstructed in the dimuon decay channel are presented in Sec.4.1. The coherent J/ψ production at central rapidities has been measured in both leptonic decays and it is described in Sec.4.2.

2.2 p-Pb collisions

In this case, the J/ψ photoproduction is dominated by the γp process and this gives the possibility to study the gluon PDF in the proton down to x∼10^{-5}. Considering the different rapidity ranges available for the measurement, ALICE

[a] e-mail: daniele.de.gruttola@cern.ch

can provide the cross section as a function of the γp center of mass energy, ranging from 21 GeV up to 1160 GeV.

3 ALICE detectors

The ALICE experiment [12] consists of a central barrel placed in a large solenoid magnet (B = 0.5 T), covering the pseudorapidity region $|\eta|$<0.9, and a muon spectrometer at forward rapidity, covering the range -4.0 <η <-2.5. The analysis at mid-rapidity makes use of the barrel detectors (SPD, TPC and TOF), the VZERO counters and the ZDC calorimeters. The Silicon Pixel Detector (SPD) makes up the two innermost layers of the ALICE Inner Tracking System (ITS). It is a fine granularity detector and can be used for triggering purposes. The Time Projection Chamber (TPC) is used for tracking and for particle identification. Beyond the TPC, the Time Of Flight detector (TOF) is used in combination with the tracking system for charged particle identification up to about 2.5 GeV/c (pions and kaons) and 4 GeV/c (protons). In addition, the TOF detector can also be used for triggering. The VZERO counters consist of two arrays (placed on opposite sides, along the beam direction, of the nominal interaction point) of 32 scintillator tiles.

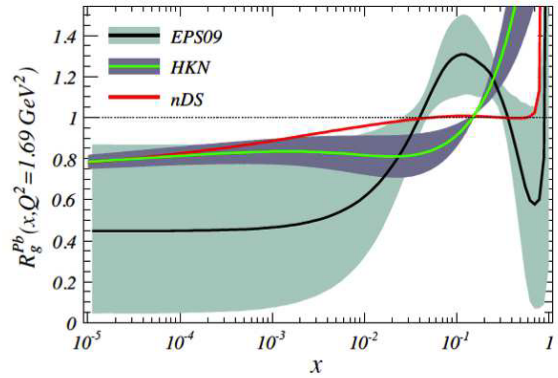

Figure 1. Ratio of their parton distribution functions for bounded and free protons vs Bjorken-x, showing ranges where shadowing, no shadowing or antishadowing are forseen.

Two sets of hadronic Zero Degree Calorimeters (ZDC) detect neutrons emitted in the very forward region such as neutrons produced by electromagnetic dissociation. The forward rapidity analyses are based on the muon spectrometer. The muon spectrometer consists of an absorber which stops hadrons but not muons in front of five tracking stations, with the third station placed inside a dipole magnet. The muon spectrometer includes a triggering system, used to select muon candidates with a transverse momentum larger than a given programmable threshold. One of the experimental challenges for the measurements presented here consists in having efficient UPC triggers. The forward UPC trigger is based on (i) the muon spectrometer trigger system, which requires the presence of an unlike sign dimuon candidate, where both tracks have p_T>0.5 GeV/c; and (ii) the VZERO trigger, which requires a signal in at least one cell in VZERO-C (muon arm side) and no signal in any cell of the VZERO-A (opposite side). The trigger for central rapidity is based on (i) at least two and less than six hits in TOF, with two of them back-to-back in azimuth, (ii) a pattern of SPD trigger signals specific for each collision system and (iii) empty VZERO detectors on both sides. The luminosity collected by UPC triggers during the 2011 Pb-Pb run was 55 μb^{-1} in the forward sample and 23 μb^{-1} in the central rapidity sample. In the p-Pb run, for the forward trigger we collected 3.9 nb^{-1} for p-Pb and 4.5 nb^{-1} for Pb-p sample.

4 J/ψ photoproduction in Pb-Pb collisions

4.1 Forward rapidity region

The dimuon invariant mass and p_T distributions for the forward region are shown in Fig.2 and Fig.3. The peak at the J/ψ mass is clearly visible and has been fitted with an exponential function to describe the background plus a Crystal Ball parameterization for the J/ψ. The clear peak at low values in the transverse momentum distribution of the J/ψ candidates is mainly due to coherent photoproduction. To estimate the fraction of incoherent events in the selected sample, a fit to the p_T distribution was performed, taking into account contributions from coherent and incoherent J/ψ production, as well as from the di-lepton continuum and the feed-down from ψ'. The shapes for these fitting functions (Monte Carlo templates) were provided by STARLIGHT events folded with the detector simulation.

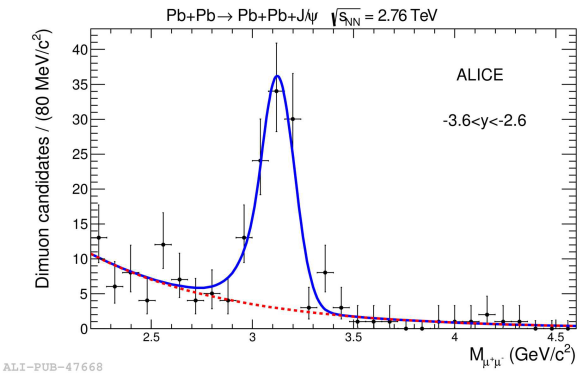

Figure 2. Invariant mass spectrum of forward (-3.6<y<-2.6) dimuons; the following cuts are applied: p_T<300 MeV/c and less than 6 neutrons in the ZDC.

As expected, at low transverse momentum the coherent production dominates. The yield of coherent J/ψ, obtained by a cut on di-muon momentum below 300 MeV/c and a ZDC cut tuned to select events with less than 6 emitted neutrons, is estimated to be $N^{coh}_{J/\psi}$=78±10(stat)$^{+7}_{-11}$(syst). The coherent differential cross section at $\sqrt{s_{NN}}$=2.76 TeV in the rapidity interval -3.6<y<-2.6 is given by:

$$\frac{d\sigma^{coh}_{J/\psi}}{dy} = \frac{1}{B.R.(J/\psi \to \mu^+\mu^-)} \frac{N^{coh}_{J/\psi}}{N_{\gamma\gamma}} \frac{(Accx\epsilon)_{\gamma\gamma}}{(Accx\epsilon)_{J/\psi}} \frac{\sigma_{\gamma\gamma}}{\Delta y}$$

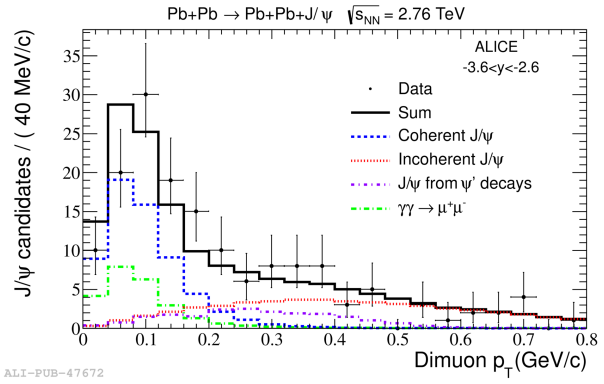

Figure 3. J/ψ p_T distribution fitted to a simulation template as described in the text.

where $B.R.$ is the branching ratio in the muon channel, Acc $\times$ ϵ is the correction for efficiency and acceptance of the coherent and continuum samples, Δy is the width of the rapidity interval and $N_{\gamma\gamma}$ is the number of $\gamma\gamma$ events in the two mass regions neighbouring the J/ψ peak; $\sigma_{\gamma\gamma}$ is the cross section for the continuum production, derived from pure QED calculation.

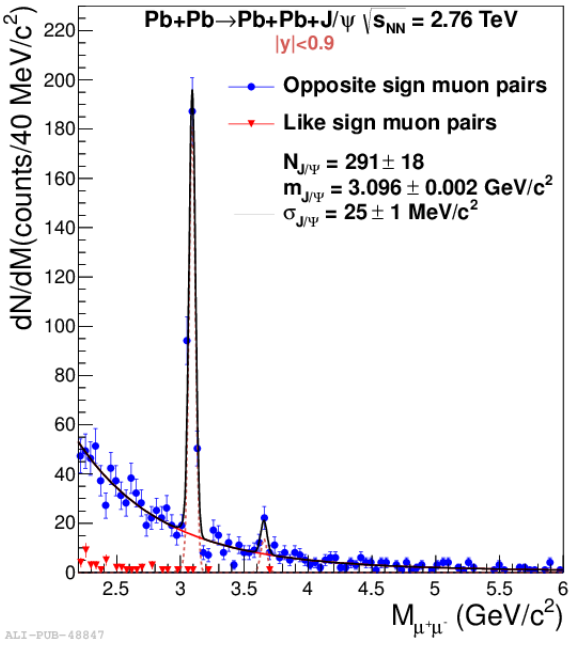

Figure 4. Invariant mass spectrum of mid-rapidity muon pairs with p_T<200 MeV/c, for events with less than 6 neutrons in the ZDC. The same distribution for the dielectron channel (with a momentum cut at 300 MeV/c) is not shown here and can be found in [14].

This cross section is known with a precision of about 20%, representing the largest source of systematic errors.

The resulting cross section is $d\sigma^{coh}_{J/\psi}/dy$ = 1.00±0.18(stat)$^{+0.24}_{-0.26}$(syst) mb.

4.2 Mid-rapidity region

In Fig. 4 the invariant mass distribution for the dimuon channel measured at mid-rapidity is shown. The data is fitted with the sum of an exponential function and two Crystal Ball functions. In the muon channel the coherence condition is applied by requiring a transverse momentum lower than 200 MeV/c. Besides the J/ψ peak, the coherent sample shows also a ψ' peak arising from the dimuon continuum. A contribution from like-sign pairs (negligible in the dielectron channel) is present in the sample corresponding to p_T>200 MeV/c and therefore enriched with incoherent events (Fig.5). It is likely to come from misidentified $\pi^+\pi^-$ pairs and it was taken into account by using a polynomial function in the corresponding fit. In the electron channel (not shown in the figure) the effects of Bremsstrahlung due to detector material are visible in the width and asymmetry of the signal, and the coherence conditions is fulfilled with a cut at 300 MeV/c. In both cases less than 6 neutrons in ZDC are required in order to suppress hadronic interactions. The transverse momentum distribution of dielectrons and dimuons can be found in [14].

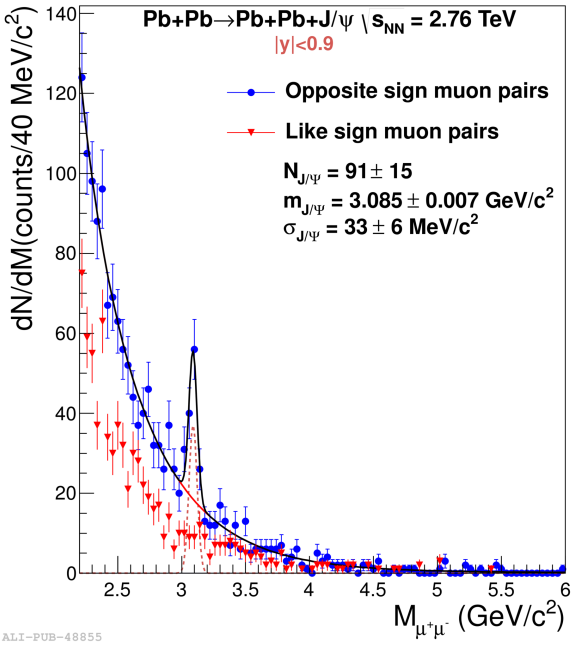

Figure 5. Invariant mass spectrum of mid-rapidity muon pairs with p_T>200 MeV/c. The same distribution for the dielectron channel (with a momentum cut at 300 MeV/c) is not shown here and can be found in [14].

To estimate the fraction of incoherent events in the selected sample, a fit to the p_T distribution was performed, taking into account the same contributions considered at forward rapidity, adding a contribution from J/ψ produced in very peripheral hadronic interactions. As for the forward rapidity analysis, the shapes for these fitting functions (Monte Carlo templates) were provided by

STARLIGHT events folded with the detector simulation.

The measured differential cross section is $d\sigma^{coh}_{J/\psi}/dy$=2.38$^{+0.34}_{-0.24}$ (stat+syst) mb.

The incoherent cross section has also been measured $d\sigma^{incoh}_{J/\psi}$/dy=0.98$^{+0.19}_{-0.17}$ (stat+syst) and compared with theoretical calculations in Fig.7.

5 Comparison of the measured cross section in Pb-Pb collisions with theoretical calculations

The results at forward and central rapidities are compared to theoretical predictions in Fig. 6. The predictions can be divided into three categories: models that include no nuclear effects (AB-MSTW08), models that use a Glauber approach for calculating the number of nucleons contributing to the scattering (STARLIGHT, GM, CSS and LM) and partonic models, where the cross section is proportional to the nuclear gluon distribution squared (AB-EPS08, AB-EPS09, AB-HKN07, and RSZ-LTA). The J/ψ photoproduction cross sections for different rapidities provide a powerful tool to constrain the nuclear gluon shadowing in the region $x \sim 10^{-3}$. The coherent J/ψ cross section is found to be in good agreement with the model which uses the nuclear gluon shadowing according to the EPS09 parameterization (AB-EPS09). Models which include no nuclear gluon shadowing are inconsistent with the measured results, as are those which use the Glauber model to incorporate nuclear effects. The AB-HKN07 and AB-EPS08 models contain too little or too much shadowing, respectively, to match the data.

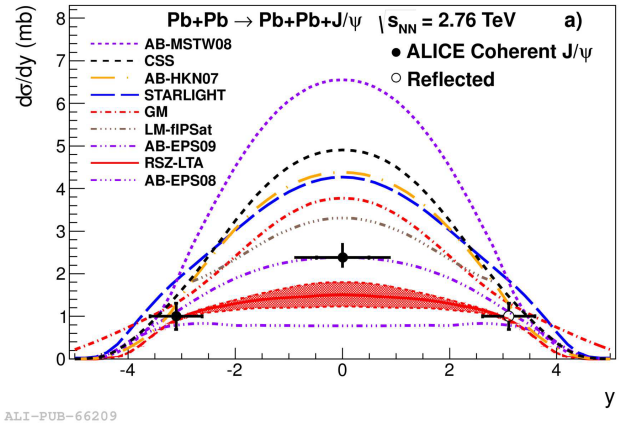

Figure 6. Comparison of the cross section at forward rapidity, at central rapidities and several theoretical models. For model references, see [14].

In Fig.7 the results of the inchoerent J/ψ photoproduction at central rapidities are compared to theoretical predictions.

Our results are about 3 sigma higher than the RSZ-LTA model prediction, although a deviation of just 1.5 sigma is found from the model upper limit. Note that the above predictions may have large uncertainties coming not only from the parametrization of the nuclear gluon

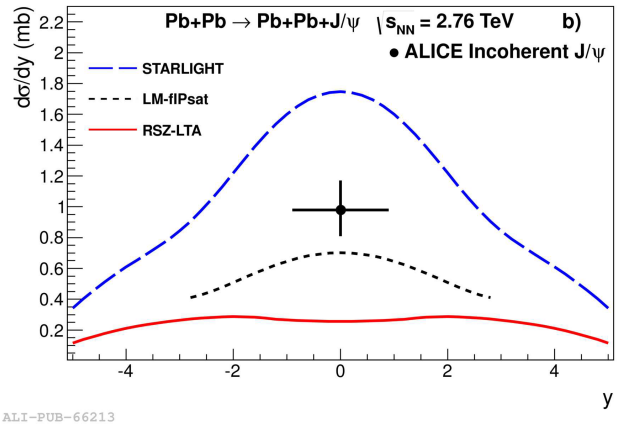

Figure 7. Comparison of the incoherent cross section at central rapidity and theoretical calculations. For model references, see [14].

distribution but also from the selection of the hard scale, the contributions from the higher-order terms, and the treatment of the photon fluctuation to a quark–antiquark pair. The current measurement will contribute to resolve these uncertainties. While none of the three existing models predicts the incoherent photoproduction cross section correctly, STARLIGHT predicts a correct incoherent-to-coherent ratio.

6 J/ψ photoproduction in p-Pb collisions

At the beginning of 2013, ALICE collected a sample of 8.4 nb^{-1} p-Pb collisions at $\sqrt{s_{NN}}$ = 5.02 TeV.

The lead nucleus acts as a photon emitter. ALICE can measure the Bjorken-x from 10^{-2} to 10^{-5}. The LHC beams were reversed in the p–Pb run; in a first period, the protons was flying towards muon spectrometer, while in the following the direction of the beams were exchanged. The J/ψ measured in the dimuon decay channel are thus reconstructed either in the 2.5<y <4.0 (p-Pb) and -3.6<y <-2.6 (Pb-p) rapidity intervals, where y is measured in the laboratory frame with respect to the direction of the proton beam. The γp center of mass energy W$_{\gamma p}$ is determined by the J/ψ rapidity: $W^2_{\gamma p} = 2E_p M_{J/\psi} e^{-y}$, where $M_{J/\psi}$ is the J/ψ mass, y is the J/ψ rapidity and E_p is the proton energy. ALICE covers the ranges 21 <$W_{\gamma p}$ <45 GeV for p-Pb and 577 <$W_{\gamma p}$ <952 GeV for Pb-p, extending the earlier measurements at HERA both to lower and to higher $W_{\gamma p}$ energies.

Fig.8 shows the invariant mass spectrum of the selected dimuons for both p-Pb and Pb-p configurations. The fit is performed by a Crystal Ball function for the signal and an exponential function for the background. The parameters of the fit are compatible with simulations of the response of the detector to this type of events. In order to extract the number of exclusive J/ψ candidates, the p_T distribution of dimuons within the J/ψ mass peak is described by 3 contributing processes, exclusive J/ψ in γp, $\gamma\gamma \to \mu^+\mu^-$ and non-exclusive J/ψ. The fits to the p_T distributions are shown in Fig.9, the shapes for exclusive J/ψ

and $\gamma\gamma \to \mu^+\mu^-$ were generated using STARLIGHT and folded with a GEANT3 detector simulation and the contribution of non-exclusive J/ψ and $\gamma\gamma \to \mu^+\mu^-$ was estimated from data.

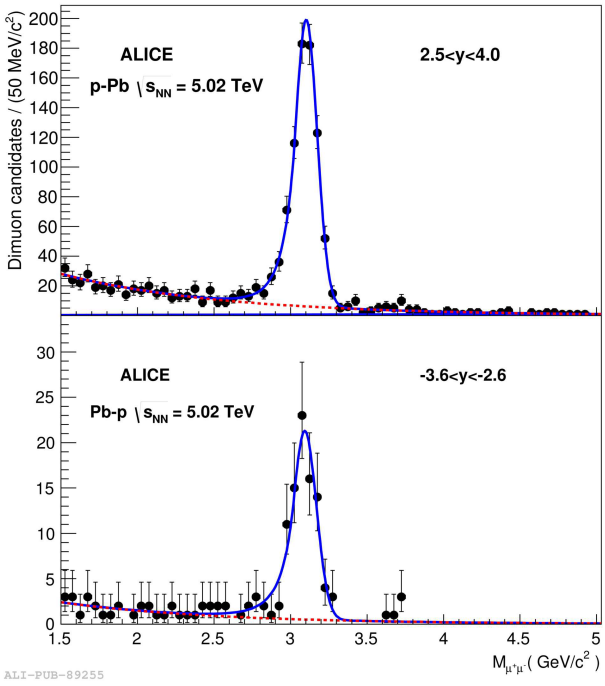

Figure 8. Invariant mass distribution for events with two oppositely charged muons, for both forward (top panel) and backward (bottom panel) dimuon rapidity samples.

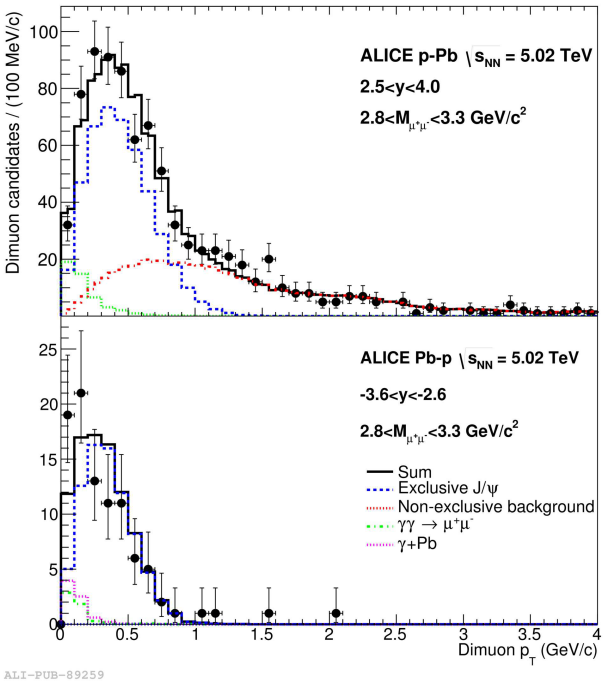

Figure 9. Transverse momentum distribution for events with two oppositely charged muons, for both forward (top panel) and backward (bottom panel) dimuon rapidity samples.

Fig.10 shows the ALICE measurements of $\sigma(W_{\gamma p})$, along with comparisons to previous measurements and to different theoretical models. In a LO pQCD approximation $\sigma(W_{\gamma p})$ is proportional to the square of the gluon PDF of the proton [17]. At HERA energies, the gluon distribution at low Bjorken-x is well described by a power law in x [18], which implies that the cross section $\sigma(W_{\gamma p})$ will also follow a power law. A deviation from such a trend in the measured cross section as x decreases, or equivalently, as $W_{\gamma p}$ increases, could indicate a change in the evolution of the gluon density function, as expected at the onset of saturation. Both ZEUS [8] and H1 [6, 7], fitted their data using a power law $\sigma \approx (W_{\gamma p})^{\delta}$, and obtained $\delta = 0.69 \pm 0.02$ (stat) $\pm$ 0.03 (syst) and $\delta = 0.67 \pm 0.03$ (stat+syst), respectively. A fit to ALICE data alone gives $\delta = 0.68 \pm 0.06$ (stat+syst).

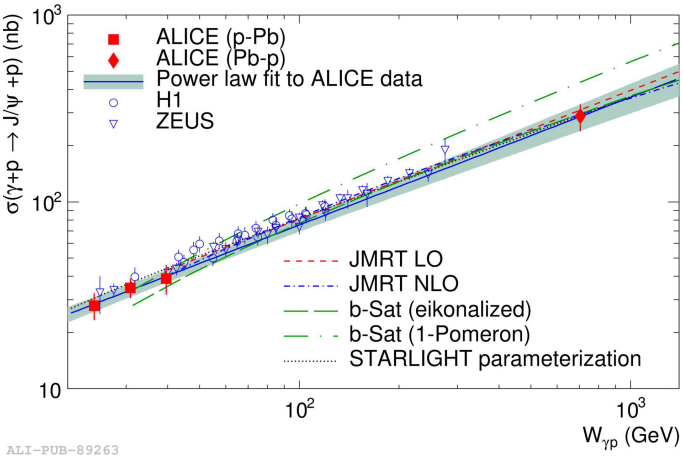

Figure 10. Comparison of the cross section at forward rapidity, at central rapidities and several theoretical models. For model references, see [19]. Only uncorrelated systematic errors were considered here.

No deviation from a power law is observed up to about 700 GeV. A natural explanation is that no change in the behaviour of the gluon PDF in the proton is observed between HERA and LHC energies.

7 Conclusions

The ALICE collaboration has made the first measurements of exclusive J/ψ photoproduction in Pb-Pb UPC. Both, the cross sections of coherent and of incoherent photoproduction of J/ψ have been measured [13, 14]. The coherent J/ψ cross section is found to be in good agreement with a model that incorporates nuclear gluon shadowing according to the EPS09 parameterization (AB-EPS09). The ALICE collaboration measured also exclusive J/ψ photoproduction off protons in p–Pb collisions at the LHC. Our data is compatible with a power law dependence of $\sigma(W_{\gamma p})$ from 20 and up to about 700 GeV in $W_{\gamma p}$, corresponding to a variation of Bjorken-x by three orders of magnitude from 10^{-2} to 10^{-5}. The slope of $\sigma(W_{\gamma p})$ determined by ALICE is consistent with the slope determined using HERA data, indicating that no change in the behaviour of

the gluon PDF in the proton is observed between HERA and LHC energies.

References

[1] E. Fermi, Nuovo Cimento 2 143-158 (1925)

[2] C. F. Weizsäcker, Z. Phys. 88 612-625 (1934)

[3] E. J. Williams, Phys. Rev. 45 729-730 (1934)

[4] A. J. Baltz et al., Phys. Rept. 458 1 (2008)

[5] C. A. Bertulani, S. R. Klein, J. Nystrand, Ann. Rev. Nucl. Part. Sci. 55 271 (2005)

[6] C. Alexa et al. [H1 Collaboration] Eur. Phys. J C 73 (2013) 2466

[7] C. Adolff et al. [H1 Collaboration] Phys. Lett. B541 (2002) 251

[8] S. Chekanov et al. [ZEUS Collaboration] Eur. Phys. J. C24 (2002) 345

[9] V. Rebyakova, M. Strikman, M. Zhalov, Phys. Lett. B 710 647 (2012)

[10] C. A. Salgado et al. J. Phys. G: Nucl. Part. Phys. 39 (2012) 015010

[11] K. J. Eskola, H. Paukkunen, C. A. Salgado, JHEP 0904 065 (2009)

[12] K. Aamodt et al. [ALICE Collaboration] , JINST 3 S08002 (2008)

[13] B. Abelev et al. [ALICE Collaboration], Phys. Lett. B 718 1273-1283 (2013)

[14] B. Abelev et al. [ALICE Collaboration], Eur. J. Phys. C 73, 2617 (2013)

[15] A. Aktas et al. Eur.Phys. J.C46:585-603,2006

[16] S. Chekanov et al., Nucl. Phys. B695 (2004) 3

[17] M. G. Ryskin, Z. Phys. C 57, 89 (1993)

[18] F. D. Aaron et al. [H1 and ZEUS Collaboration], JHEP 1001, 109 (2010)

[19] B. Abelev et al. [ALICE Collaboration], arxiv:1406.7819, accepted for publication in PRL